ELSEVIER

Catalysis Today 66 (2001) 145–155

CATALYSIS TODAY

www.elsevier.com/locate/cattod

Dynamic methods and new reactors for liquid phase molecular catalysis

Sylvain Caravieilhes, Claude de Bellefon*, Nathalie Tanchoux

Laboratoire de Génie des Procédés Catalytiques, CNRS/ESCPE Lyon, Bâtiment 308, 43 Bd du 11 Novembre 1918, BP 2077, F-69616 Villeurbanne, France

Abstract

Kinetic data acquisition and screening of transition metal complexes for *homogeneous* liquid phase catalysis calls for numerous testing in multiphase G/L, L/L and G/L/L systems. It is shown first, with an example in asymmetric hydrogenation, why detailed kinetics must be performed. Then, new reactors leading to fast experimental techniques are proposed. A liquid–liquid centrifugal partition chromatography is evaluated for determining rate constants and partition isotherms by combining frontal analysis and elution chromatography, the catalyst being maintained in a stationary aqueous phase. Two microreactors offering short residence time have also been tested and compared with a fast test reaction (t_R ca. 5–20 s). The combination of reacting pulses, carrier liquids and micromixer is proposed as a general high throughput tool for the investigation of G/L, L/L and G/L/L catalytic systems in a fast sequential way.

Keywords: Liquid–liquid catalysis; Kinetics; Mass transfer; Microreactors; Chromatographic reactor

1. Introduction

Today, numerous research groups are focusing their activities on the synthesis of transition metal complexes that may be used as catalysts. New synthetic methodologies having high throughput capabilities such as combinatorial chemistry are now applied to the synthesis of transition metal complexes which will ultimately lead to huge libraries of ligands hence of catalyst precursors [1–3]. Testing of these catalyst precursors in *one liquid phase* does not represent a problem as long as the reactions are not too fast compared with micromixing [4,5,27]. Screening apparatus have been developed that fulfil the requirement of ensuring meaningful and reproducible tests on microquantities of samples to be investigated that are produced by the combinatorial techniques.

However, numerous reactions such as hydrogenations, carbonylations, hydroformylations are operated in gas–liquid systems. Furthermore, in order to solve the problem of catalyst separation and recycling, new technologies aiming at dissolving the catalyst in a third non-miscible liquid phase are developed [6].

New triphase gas/liquid/liquid catalysis emerged where one of the liquid phase is an organic layer that only contains the substrate(s) and product(s). This is the actual basis for the Ruhrchemie–Rhône–Poulenc hydroformylation G/L/L process, where the catalyst resides in an aqueous layer [7]. Other technologies include ionic liquids [8] and fluorocarbons media [9] to trap the catalyst.

The challenging problem for chemical engineers in this field is to develop or to adapt tools for catalysts

* Corresponding author. Tel.: +33-472-431-754; fax: +33-472-431-673.
E-mail addresses: cdb@lgpc.cpe.fr, cdb@lobivia.cpe.fr (C. de Bellefon).

0920-5861/01/$ – see front matter
PII: S0920-5861(00)00615-5

Nomenclature

C_{Aq}	concentrations in the aqueous phase (kmol m_{Aq}^{-3})
$C_{Aq}^{DMI\ in}$	concentration of DMI in the aqueous phase (kmol m_{Aq}^{-3}) at the microreactor inlet
C_{Org}	concentrations in the organic phase (kmol m_{Org}^{-3})
$C_{Org}^{DMI\ in}$	concentration of DMI in the organic phase (kmol m_{Org}^{-3}) at the microreactor inlet
k	intrinsic kinetic constants (m_{Aq}^3 $kmol^{-1}$ s^{-1})
k_1a	volumic mass transfer coefficient (s^{-1})
K	inhibition constants in intrinsic kinetic rate models (m_{Aq}^3 $kmol^{-1}$)
N	number of perfectly mixed reactors in the cascade reactor model (–)
p^A	empirical parameter for the partition isotherms of species A (m_{Org}^3 $kmol^{-1}$)
P_A	partition coefficient of species A between the organic and the aqueous phases, $P_A = C_{Org}^A/C_{Aq}^A$ (m_{Aq}^3 m_{Org}^{-3})
Q_{Aq}	volumic flow rate of the mobile aqueous phase (m_{Aq}^3 s^{-1})
Q_{Org}	volumic flow rate of the mobile organic phase (m_{Org}^3 s^{-1})
r_{Aq}	rate of the reaction per unit volume of the aqueous catalytic phase (kmol m_{Aq}^{-3} s^{-1})
r_{Org}	observed rate of the reaction per unit volume of the organic phase (kmol m_{Org}^{-3} s^{-1})
V_{Aq}	volume of the aqueous phase (m_{Aq}^3)
V_{Column}	total volume of the column in the CPC reactor (m^3)
V_{Org}	volume of the organic phase (m_{Org}^3)

Superscripts and subscripts

A	superscript related to substrates
BZA	superscript and subscript related to the substrate benzaldehyde
BZOH	superscript and subscript related to the product benzylic alcohol
DMI	superscript related to the substrate dimethylitaconate
HCOO	superscript related to sodium formate
k	increment number of perfectly mixed reactors in the cascade reactor model (subscript)
P	superscript related to the ligand triphenylphosphinetrisulphonated, sodium salt
Rh	superscript related to rhodium
Ru	superscript related to ruthenium

Greek letters

α	volumic ratio of the organic phase and the aqueous phase (m_{Org}^3 m_{Aq}^{-3})
θ	pulse duration in the transient experiments in the CPC reactor (s)
τ	residence time in one of the perfectly mixed reactor in the cascade reactor model, $\tau = (V_{column}/N)/Q_{Org}$ (s)
χ	molar conversion (–)

screening that would ensure meaningful and reproducible tests on microquantities of samples and under polyphasic conditions.

In keeping with this goal, we have used a new liquid–liquid plug flow reactor as well as microreactors for catalyst testing and kinetic studies. This report describes our results concerning liquid–liquid catalytic reactions including modelling of chemical kinetics, model discrimination, thermodynamic data determination and mass transfer evaluation. Selected examples are provided in the following sections.

2. Chemical kinetics

How far can a mechanism be used to build a realistic rate law? Lot of very detailed but not so proved mechanisms are available in the literature of molecular catalysis [6,10]. Using the steady-state approximation on the catalytic intermediates, kinetic models can be derived from the elementary steps of such mechanisms. However, this procedure often drives to rate laws displaying a large number of constants. In

such cases, kinetic parameter estimation and model discrimination cannot be performed unambiguously. Conversely, from global kinetic measurements, how far can elementary steps, based on the knowledge of organometallic chemistry, be postulated? These aspects have been discussed in a previous report for the asymmetric reduction of acetophenone into phenylethanol [11].

Here, the asymmetric hydrogenation of *Z*-methylacetamidocinamate by the Rh(dipamp) catalyst [12] will exemplify this approach. The kinetic laws for the production of the *R* and *S* enantiomers of the product are given in Eqs. (1) and (2):

$$r_R = \frac{k_{1r}k_{2r}C_{Rh}C_{MAC}C_H}{(k_{-1r}+k_{2r}C_H)(1+(k_{1r}C_{MAC}/(k_{-1r}+k_{2r}C_H))+(k_{1s}C_{MAC}/(k_{-1s}+k_{2s}C_H)))} \quad (1)$$

$$r_S = \frac{k_{1s}k_{2s}C_{Rh}C_{MAC}C_H}{(k_{-1s}+k_{2s}C_H)(1+(k_{1r}C_{MAC}/(k_{-1r}+k_{2r}C_H))+(k_{1s}C_{MAC}/(k_{-1s}+k_{2s}C_H)))} \quad (2)$$

where C_H, C_{Rh} and C_{MAC} are, respectively, the hydrogen, catalyst and substrate concentrations. As depicted, up to six constants corresponding to the six rate-limiting elementary steps of the mechanism have to be determined. That has been performed by Halpern and Landis using the methodology of co-ordination chemistry, looking at each step independently with powerful spectroscopic techniques. However, this approach only applies to catalytic reactions where the catalytic intermediates are nice enough to accumulate during the catalysis and when spectroscopic tools such as ^{31}P NMR may operate. The numerical values for the parameters at 25°C are: k_{1R} 318 000 ($m^3\,kmol^{-1}\,min^{-1}$), k_{1S} 636 000 ($m^3\,kmol^{-1}\,min^{-1}$), k_{-1R} 9 (min^{-1}), k_{-1S} 192 (min^{-1}), k_{2R} 66 ($m^3\,kmol^{-1}\,min^{-1}$) and k_{2S} 37 800 ($m^3\,kmol^{-1}\,min^{-1}$).

Out of the 10 experiments at 25°C reported by Halpern, six have been chosen. That set of experiments well reflects the range of the operating conditions (hydrogen pressure/concentration, catalyst and substrate concentrations). The published kinetic constants were used to generate global kinetic data and computer-generated noise was added to provide pseudo-experimental concentration vs. time profiles (Fig. 1).

The parameter estimation can be conducted with only one or all the six experiments. When two experiments are used, two out of six combinations of experiments are achievable that drives to 14 kinds of parameters estimations. Obviously, these 14 estimations will provide slightly different sets of kinetic parameters. For three experiments used, the same calculation gives 20 estimations. For four, five and six, respectively, nine, six and one estimations can be run. Fig. 2 shows the results for some selected kinetic parameters.

Considering the two kinetic parameters, k_{-1S} and k_{2R} (Fig. 2a and b), a rather trivial conclusion is that when, the more the experiments are used, the more accurate is the estimation. The same is true for k_{-1R} and k_{2S} which are perfectly determined. However, the kinetic parameters k_{1R} and k_{1S} cannot be determined,

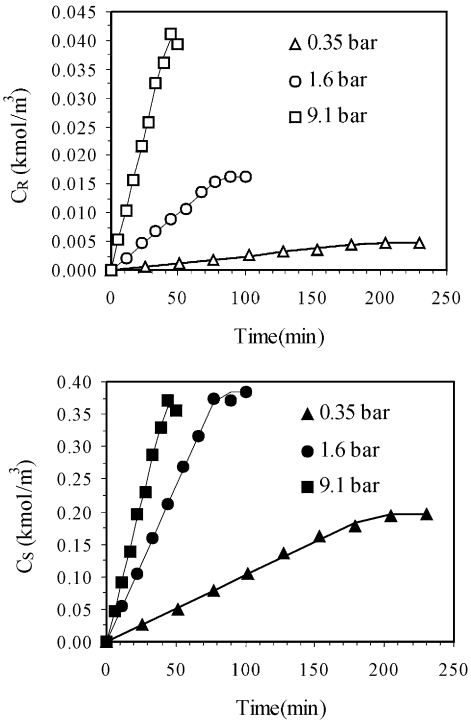

Fig. 1. Computed pseudo-experimental (a) R and (b) S products concentration vs. time profiles for experiments at three selected hydrogen pressure. The lines represent the theoretical profiles.

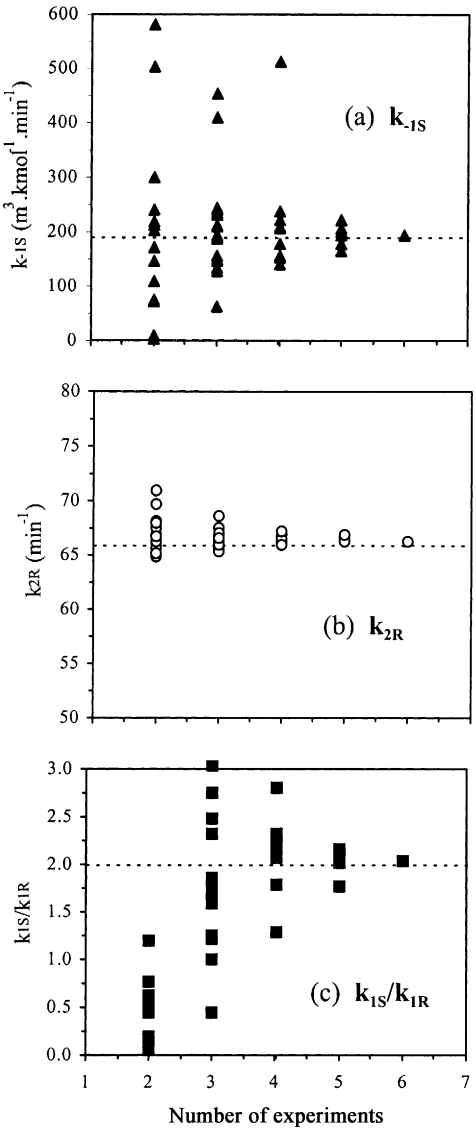

Fig. 2. Influence of the number of experiments used on the discernability of three selected kinetic parameters: (a) k_{-1S}; (b) k_{2R}; (c) k_{1S}/k_{1R}.

irrespectively, of the number and the nature of the experiment sets chosen. On the contrary, their ratio k_{1S}/k_{1R} is very well determined with five or six experiments (Fig. 2c).

Thus, within the experimental conditions used by Halpern, considering a realistic experimental (analytical) error of 3%, up to five parameters (k_{-1R}, k_{-1S}, k_{2R}, k_{2S} and k_{1S}/k_{1R}) out of six can be determined with global kinetic measurements. Can all set of the six kinetic parameters be experimentally fully determined? The mathematics say yes, because the rate models are perfectly discernible. A further experiment can be designed to determine k_{1S} and k_{1R} unambiguously. The computed operating conditions are $C_{MAC} = 0.003\,\text{kmol}\,\text{m}^{-3}$ and $P_{H_2} = 10\,\text{MPa}$ which seems not so unrealistic for a *real* experiment.

Now comes the key question: Is it so useful to determine the full set of kinetic parameters? Does the design of an industrial asymmetric hydrogenation process to require such level of details?

The literature is very scarce on such data. On one hand, very detailed kinetic modelling have been reported from researchers at Novartis on a Pt/alumina/cinchonidine asymmetric hydrogenation catalyst [13,14]. On the other hand, a recent paper reports the scale-up of an asymmetric hydrogenation with a very similar catalyst in which the metal is Ru instead of Rh in the previous example [15]. The intrinsic kinetic was very simple, just used to describe the rate of hydrogen consumption. The selectivity (enantioselectivity) was considered and shown to be very little sensitive to the operating conditions, particularly to the hydrogen pressure. This is, however, in no way a general rule! For Rh-based enantioselective hydrogenation catalysts, the enantioselectivity does depend on the liquid phase hydrogen concentration [16]. The impact of the coupling of such intrinsic kinetics with gas–liquid mass transfer resistances on the enantioselectivity has been theoretically analysed and shown to be far from negligible [17].

Besides these scale-up considerations, one should realise that the quantification of the rate constants of elementary mechanistic steps may drive to the understanding of the factors governing the chiral induction at the catalytic site. The determination and tabulation of such data is indeed a scientific challenge which remains to be solved.

Because numerous data must be collected, it also calls for new methodologies. Just for rhodium-based catalysts and considering only commercially available phosphine-type chiral inductors, more than 30 catalysts can be prepared. The number of substrates that can be reduced by asymmetric hydrogenation is considerably higher. That number must then be combined with a range of operating conditions which will probably lead to a huge number of experiments to be

Table 1
Conditions for kinetic study in the batch reactor

Temperature (K)	303–333
Initial BZA concentration in the organic phase, $C_{Org}^{BZA\,o}$ (kmol m_{Org}^{-3})	0.05–0.2
Initial BZA concentration in the aqueous phase, $C_{Aq}^{BZA\,o}$ (kmol m_{Org}^{-3})	0.014 à 0.06
Organic phase volume, V_{Org} (cm^3)	20
Volume ratio, α ($m_{Org}^3\, m_{Aq}^{-3}$)	0.1–0.2–1
Ru concentration, C_{Aq}^{Ru} (mol m_{Aq}^{-3})	3.4–9.5

performed. It is obvious that existing methods and reactors are not well designed for such a task. During the course of our study on kinetics of asymmetric catalytic reductions, we have developed methods and reactors that can fulfil these requirements.

3. Transient operations in a centrifugal partition chromatograph (CPC)

3.1. Reaction, kinetics and liquid–liquid partition

The catalytic H-transfer reduction of benzaldehyde (BZA) into benzylic alcohol (BZOH) with sodium formate, catalysed by a water soluble ruthenium complex in a biphasic cyclohexane–water mixture was chosen as a test reaction (Eq. (3)). Analysis of the organic layer and mass balance calculations confirm the stoichiometry of Eq. (3), no side products being detected:

$$C_6H_5CHO + HCO_2Na + H_2O \rightarrow C_6H_5CH_2OH + NaHCO_3 \quad (3)$$

The kinetic measurements were performed in a well-mixed batch reactor (100 cm^3). The rate of reaction was independent of the mixing speed above 600 rpm which supports the absence of mass transfer limitations under the conditions of the experiments (1100 rpm). In a typical experiment, an aliquot of the catalyst (ca. 2 cm^3) was added to a mixture of a solution of sodium formate (5 M) in water, cyclohexane, BZA (40 ml total volume). The reaction began immediately and the concentrations of the BZA and benzyl alcohol in the organic layer were followed by gas chromatography. The range of the operating conditions for the kinetic measurements are given in Table 1.

Kinetic model discrimination leads to the empirical intrinsic rate of reaction (Eq. (4)):

$$r_{Aq} = \frac{kC_{Aq}^{Ru}C_{Aq}^{BZA}}{1 + K^{Ru}C_{Aq}^{Ru} + K^{BZA}C_{Aq}^{BZA}} \text{ (kmol } m_{Aq}^{-3}\, s^{-1}) \quad (4)$$

The BZA concentrations being measured in the organic layer, the rate is more usefully expressed with respect to C_{Org}^{BZA}. Mass balance in the batch reactor drives to the observed empirical rate law (Eq. (5)):

$$r_{Org} = \frac{kC_{Aq}^{Ru}C_{Org}^{BZA}}{(1 + \alpha P_{BZA})(1 + K^{Ru}C_{Aq}^{Ru} + (K^{BZA}/P_{BZA})C_{Org}^{BZA})} \quad (5)$$

where r_{Org} is in kmol $m_{Org}^{-3}\, s^{-1}$, $P_{BZA} = C_{Org}^{BZA}/C_{Aq}^{BZA}$, and $\alpha = V_{Org}/V_{Aq}$. Here k is the kinetic constant, K^{Ru} and K^{BZA} are inhibition constants and P_{BZA} the partition coefficient of BZA between the organic and the aqueous phase (measured 50). The latter coefficient is estimated from the partition isotherm which is approximately linear in the concentration range used for the experiments. The goodness of fit for the rate law of Eq. (5) is shown in Fig. 3.

The kinetic parameters k, K^{Ru} and K^{BZA} were estimated with a specially designed computer software [18] from the full concentration vs. time profiles of 30 experiments obtained under a broad range of operating conditions (Table 2).

3.2. Theoretical of the CPC

In liquid–liquid biphasic catalysis, concentration vs. time profiles as those recorded batchwise imply that a fresh batch of catalyst is used for each of the kinetic experiments. Indeed, after an experiment, the catalytic layer contains the product(s) of reaction. Recycling of the catalyst would involve multi-extraction and

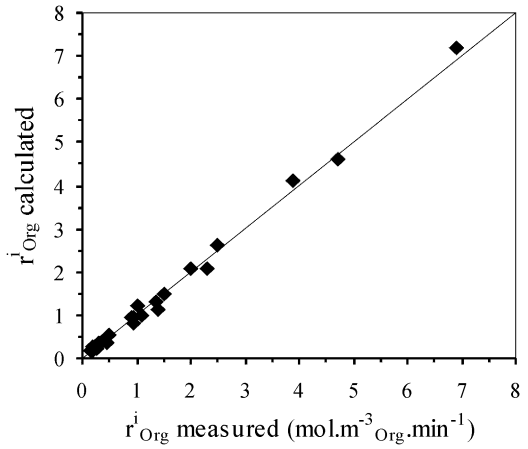

Fig. 3. Parity plot of the observed vs. experimental initial rate of reaction for the 30 experiments used.

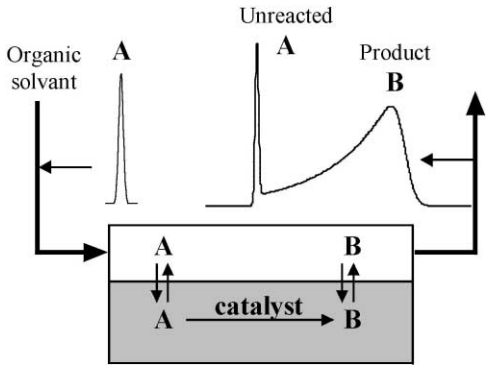

Fig. 4. Schematic diagram of the transient operation in the CPC.

washing of the aqueous phase. Such a procedure is often referred in the field of homogeneous catalysis as detrimental for the catalyst.

The CPC reactor offers a way to collect similar profiles using transient operations on the mobile phase (the organic layer), the catalyst being trapped as a stationary phase (aqueous layer) in the column [21]. A schematic diagram of the transient operation is depicted in Fig. 4.

The aqueous catalytic phase is the stationary phase and an organic solvent is the carrier mobile phase. At a certain time, the substrate is injected via an injection valve. Because the partition coefficients of A and that of B are quite different, the product B will separate from the substrate A all along the column. At the exit of the CPC, the shape of the peak of the product should not only reflect the efficiency of the chromatograph, as usually found in chromatography, but also the kinetics of the reaction.

Table 2
Estimated kinetic constants and statistical analysis

Parameter	Value	Confidence interval[a]
k_{323} (m^3_{Aq} $kmol^{-1}$ s^{-1})	2820	2590–3070
E_a (kJ mol^{-1})	109	107–111
K^{Ru} (m^3_{Aq} $kmol^{-1}$)	1320	1100–1540
K^{BZA} (m^3_{Aq} $kmol^{-1}$)	21	18–24

[a] Interval at 95% confidence level. The WRSS (weighted residuals sum of squares) is 55.

A model has been developed for fluid/solid chromatography by Villermaux [19,28] in the case of an ideal plug flow system, in the absence of mass transfer limitation, for linear partition isotherm of the chemicals between the two liquid phases and for first-order kinetics. Application of this model to the case of liquid–liquid systems looks promising.

3.3. Transient run in the CPC reactor

The volume, length and inner diameter of the column are, respectively, 55 cm^3, 17 m and 0.15 cm. A speed of revolution of 750 rpm was imposed in order to maintain the catalytic aqueous layer trapped in the column. Each elementary volume of the coiled column describes an epicycloidal trajectory and is exposed to a centrifugal force field whose direction changes constantly. That insures the two liquid phases to be alternatively mixed and separated all along the coiled part of the column. Further references on the basic understanding of CPC-type apparatus can be found in [20].

After equilibration, cyclohexane is pumped through the column at 0.5–2 cm^3 min^{-1} flow rate. At this stage, pulses of BZA, typically 0.2 cm^3 of 0.1 M solutions in cyclohexane, were injected at the inlet of the column. At the outlet of the apparatus, the organic phase was sampled and analysed by gas chromatography.

Previous studies based on residence time distribution analysis have shown that plug flow can be considered in the CPC reactor with Péclet numbers in the range 200–2000 and that mass transfer is not limiting for the catalytic systems used [22,29].

A model with N perfectly mixed reactors, open to the mobile organic phase, has been designed with no mass transfer limitations and where the specific rate of chemical production is given by Eq. (4). In reactor k, the mass balance equations for the substrate BZA and the product benzyl alcohol (BZOH) as well as the boundary conditions are given in Eqs. (6) and (7):

$$\frac{1}{\tau}(C^{\mathrm{BZA}}_{\mathrm{Org}\,k-1} - C^{\mathrm{BZA}}_{\mathrm{Org}\,k}) = \frac{1+\alpha P_{\mathrm{BZA}}}{(1+\alpha)P_{\mathrm{BZA}}}\frac{\mathrm{d}C^{\mathrm{BZA}}_{\mathrm{Org}\,k}}{\mathrm{d}t} + \frac{1}{1+\alpha}r_{\mathrm{Aq}} \quad (6)$$

$$\frac{1}{\tau}(C^{\mathrm{BZOH}}_{\mathrm{Org}\,k-1} - C^{\mathrm{BZOH}}_{\mathrm{Org}\,k}) = \frac{1+\alpha P_{\mathrm{BZOH}}}{(1+\alpha)P_{\mathrm{BZOH}}}\frac{\mathrm{d}C^{\mathrm{BZOH}}_{\mathrm{Org}\,k}}{\mathrm{d}t} - \frac{1}{1+\alpha}r_{\mathrm{Aq}} \quad (7)$$

where $\tau = V_{\mathrm{Column}}/NQ_{\mathrm{Org}}$ is the reduced residence time.

Boundary conditions:

$$C^{\mathrm{BZOH\,o}}_{\mathrm{Org}} = 0 \quad \forall t$$

and

$$C^{\mathrm{BZA\,o}}_{\mathrm{Org}} = \begin{cases} C^{\mathrm{BZA\,o}}_{\mathrm{Org}} & \text{for } 0 \le t \le \theta, \\ 0 & \text{otherwise} \end{cases}$$

Based on the model, a home-made Fortran code has been used for the simulation of the experimental results. Fig. 5 depicts the goodness of fit obtained *without parameter fitting*.

The difference observed between the experimental points and the model is attributed to partition coefficient rather than to the kinetic parameters. Indeed, it is likely that the product benzyl alcohol which is quite water soluble acts as a co-solvent for the less water soluble benzaldehyde.

Thus, this technique requires the accurate determination of the liquid–liquid partition isotherms for both reagents and under reaction conditions. A method, based on chromatographic separation in the CPC, has been developed.

3.4. Determination of liquid–liquid partition isotherms

As mentioned, one particular problem in biphasic catalysis is to describe the partition of the substrate and products between the organic and the catalytic (aqueous) layer. Some of these thermodynamic data for ternary and quaternary mixture are available from the literature or from calculations.

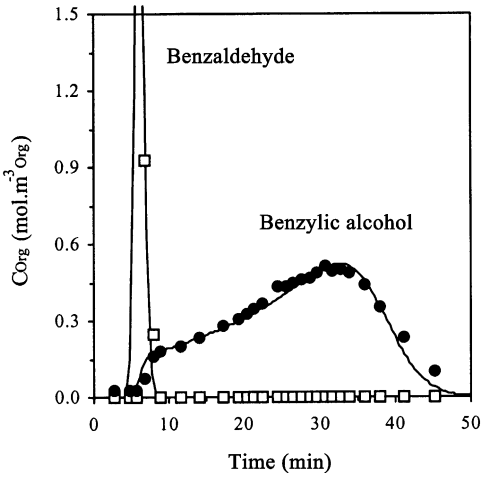

Fig. 5. Comparison between the experiment and the model without fitting parameters. Conditions: 323 K; $Q = 1\,\mathrm{cm^3\,min^{-1}}$; $C^{\mathrm{Ru}}_{\mathrm{Aq}} = 0.01\,\mathrm{kmol\,m^{-3}_{Aq}}$; $C^{\mathrm{BZA\,o}}_{\mathrm{Org}} = 0.1\,\mathrm{kmol\,m^{-3}_{Org}}$; $V_{\mathrm{Column}} = 55\,\mathrm{cm^3}$; $\alpha = 0.14$. Experiments (symbols) and model (lines) ($N = 100$).

However, it is very often found that the nature of the catalytic phase being used is too far from, e.g. pure water, due to the presence of the catalyst itself. Thus, in practice, liquid–liquid partition measurements are performed which are time consuming.

A dynamic method, first developed in gas–solid chromatography [23], was adapted to liquid–liquid systems in the CPC. The method operates in two steps: (1) equilibration of the stationary phase with continuous feeding of the mobile phase containing

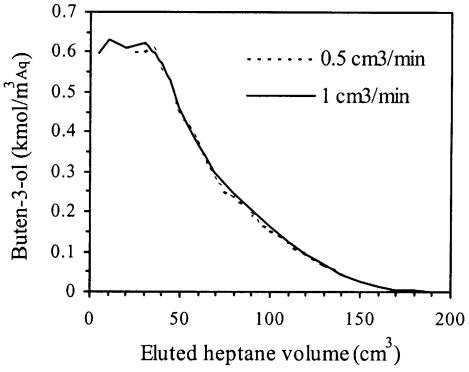

Fig. 6. Chromatograms for buten-3-ol for two flow rates showing no mass transfer limitations.

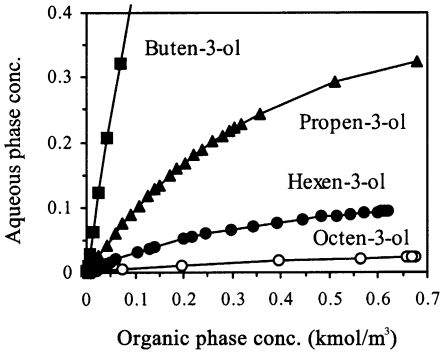

Fig. 7. Water/*n*-heptane partition isotherms for C_4 to C_8 allyl alcohols.

the solute, and (2) switching of the feed flow to pure solvent in order to obtain a desaturation front in the chromatogram (Fig. 6).

Working-up of these chromatograms assuming a mass balance as indicated in Eqs. (6) and (7) but without chemical production terms leads to liquid–liquid partition isotherm curves. Water/*n*-heptane partition isotherms for a series of allyl alcohols were determined (Fig. 7).

These isotherms can be fitted with functions as indicated in Eq. (8) where q^A and p^A are empirical parameters:

$$C^A_{Aq} = \frac{q^A C^A_{Org}}{1 + p^A C^A_{Org}} \,(\text{kmol m}^{-3}_{Aq}) \tag{8}$$

That can then be used in place of constant partition coefficients that are valid only in dilute solutions. In summary, this method proves to be fast, accurate and easy to automatise. Further works are in progress to determine isotherms for more complex mixtures.

4. Microreactors for liquid–liquid catalysis

The use of microreactors for liquid–liquid reactions may present definitive advantages. Just to list some, it allows short residence time, possesses high heat exchange capabilities. In the case of biphasic catalysis with expensive molecular catalysts, it also leads to less catalyst consumption hence providing a good tool for catalyst screening.

Two microdevices were tested. The first allows residence time up to some minutes but was designed for exothermic reactions rather than for efficient mass transfer [24,30]. The other is a micromixer optimised for mixing but offering residence time of only some seconds [25,31].

4.1. Mass transfer evaluation in a microreactor

The estimation of the global liquid–liquid mass transfer coefficient k_1a was performed with a chemical reaction of well-known kinetics. The liquid–liquid H-transfer reduction of dimethylitaconate (DMI) into dimethylmethylsuccinate (DMS) with sodium formate catalysed by a water soluble rhodium phosphine catalyst was studied previously in our laboratory [29] and drove to the following rate law (Eq. (9)):

$$r_{Aq} = \frac{kC^{Rh}_{Aq}C^{DMI}_{Aq}}{KC^{DMI}_{Aq} + C^{HCOO}_{Aq}C^{P}_{Aq}} \,(\text{kmol m}^{-3}_{Aq}\,\text{s}^{-1}) \tag{9}$$

The microreactor bears 32 microchannels arranged in four sets of eight microchannels. A picture of one of these sets is shown in Fig. 8.

The mixing of the two liquid phases is ensured by a simple microgrid. After circulation in the microchannels, the L/L mixture is collected through microchannels with larger section computed to maintain a constant flow velocity. The total volume of the contact zone is $0.345\,\text{cm}^3$. The four microelement plates are then mounted and sandwiched between stainless steel seal equipped plates that bear the inlet and outlet pipes (Fig. 9).

The results show that whereas conversion close to 90% are expected from the intrinsic kinetics and from control batch experiments, only 43% is achieved in the microreactor (Fig. 10).

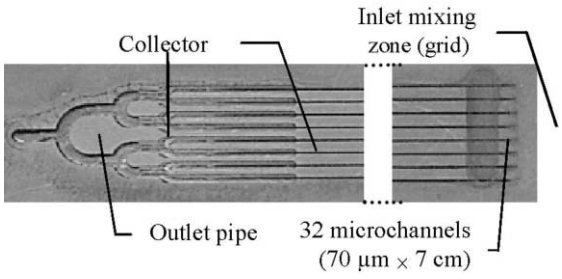

Fig. 8. One of the four microelement picturing the tree-shaped collector (courtesy of IMM).

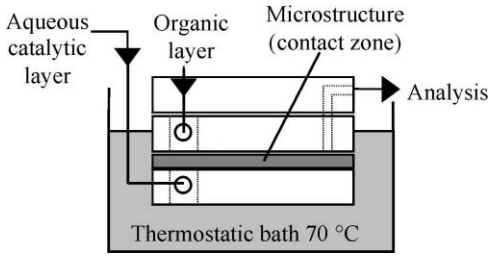

Fig. 9. Experimental set-up for the catalytic tests in the multichannel microreactor.

In order to account for the experimental results, a liquid–liquid mass transfer resistance has been introduced. The following model includes the intrinsic kinetics as in Eq. (9) and a global mass transfer coefficient k_1a, for the reaction DMI → DMS and assuming no axial dispersion (Scheme 1).

Mass balance for the aqueous layer:

$$k_1 a \left(\frac{C^{\mathrm{A}}_{\mathrm{Org}}}{P_{\mathrm{A}}} - C^{\mathrm{A}}_{\mathrm{Aq}} \right) \mathrm{d}V_{\mathrm{Aq}} + r_{\mathrm{Aq}} \, \mathrm{d}V_{\mathrm{Aq}} = Q_{\mathrm{Aq}} \, \mathrm{d}C^{\mathrm{A}}_{\mathrm{Aq}} \tag{10}$$

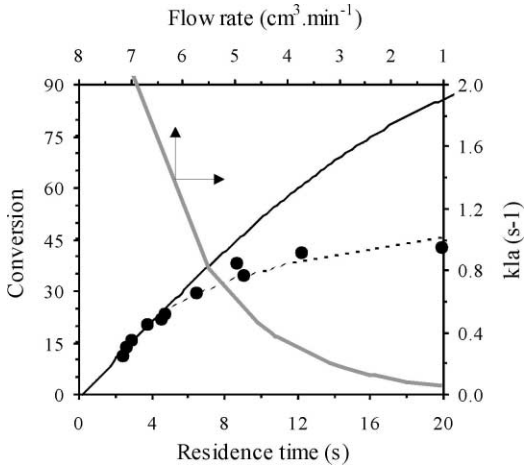

Fig. 10. Experimental results vs. models. Main axis: experimental conversions (●); intrinsic kinetic model (–); kinetic model + mass transfer resistance (- - - -). Secondary axis: variation of computed k_1a with flow rates (—). Conditions: $Q_{\mathrm{Org}}/Q_{\mathrm{Aq}} = 0.5$; 70°C; organic layer, cyclohexane; aqueous layer, sodium formate 1 M with $C^{\mathrm{Rh}}_{\mathrm{Aq}} = 4.5\,\mathrm{mol\,m^{-3}}$. The Rh catalyst and the formate are not cyclohexane soluble. Inlet conditions: $C^{\mathrm{DMI\,o}}_{\mathrm{Org}} = 0.05\,\mathrm{kmol\,m^{-3}}$, and $C^{\mathrm{DMI\,o}}_{\mathrm{Aq}} = 0$.

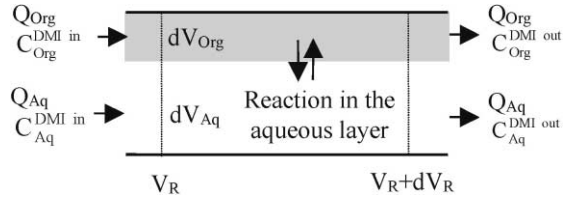

Scheme 1. Reactor model.

Mass balance for the organic layer:

$$-k_1 a \left(\frac{C^{\mathrm{A}}_{\mathrm{Org}}}{P_{\mathrm{A}}} - C^{\mathrm{A}}_{\mathrm{Aq}} \right) \mathrm{d}V_{\mathrm{Aq}} = Q_{\mathrm{Org}} \, \mathrm{d}C^{\mathrm{A}}_{\mathrm{Org}} \tag{11}$$

The mass transfer coefficient k_1a is the only fitting parameter. The result of the fit is pictured in Fig. 10. For each data point, a mass transfer coefficient is estimated. An increase of the computed k_1a with the flow rate is noticed which is attributed to a better static mixing effect of the grid at higher flow rates.

4.2. A micromixer to ensure chemical regime

A static micromixer available from the IMM institute was used. A picture of the microdevice is shown in Fig. 11. The two liquid phase inlets are *in the plane* of the drawing. A discharge slit (60 μm × 4 mm), located above and perpendicular to the interdigitated channels collects the mixture.

The experimental set-up consists in the mounting of the micromixer at the inlet of a simple stainless steel tube (4 mm i.d.) that ensures the desired residence time. Again, the liquid–liquid reduction of dimethyli-

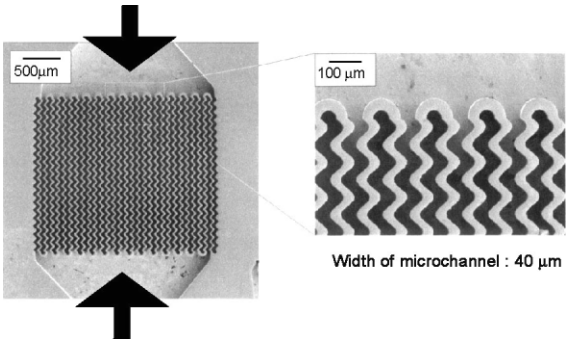

Fig. 11. SEM images of a mixing element: 2 × 15 interdigitated microchannels with corrugated walls (courtesy of IMM).

taconate (DMI) into dimethylmethylsuccinate (DMS) was the test reaction.

Preliminary results indicate that conversions up to 80% are achieved with the use of the micromixer, under the same reaction conditions as described in Fig. 10. However, the micromixer presents one drawback: the quality of the liquid–liquid emulsion is very much sensitive to the flow rate. Hence, flow rates above 6 cm^3 min^{-1} must be used in order to maintain the chemical regime. For a range of residence time compatible with the reaction (up to 30 s), such flow rates drive to reactor volumes of more than 2 cm^3, for which coalescence may drive to mass transfer limitations, hence counterbalancing the mixing efficiency.

5. Conclusion and future works

The methods presented so far have not solved the problem of catalyst availability. For both the CPC and the microreactors, large quantities of catalysts are required. In the CPC, ca. 30 cm^3 of the aqueous catalyst is used which represents ca. 200 mg catalyst. The same is true for the microreactors which operate under steady-state conditions with quite large flow rates. A trivial thought is to operate the microreactors in a transient mode. A basic set-up for that is shown in Fig. 12.

That should offer definite advantages over the previous methods. Micropulses containing microquantities of both the catalyst and the substrate will be used. Changing or adapting the micromixer would allow the introduction of reacting gas for the study of G/L catalytic reactions. Serial mounting of the microdevices will drive to G/L/L microreactors with perfectly controlled residence time, mixing, hold-up and temperature. Preliminary qualitative results in our hands support this view albeit revealing that quantitative data will require robust modelling of these new reactors [26].

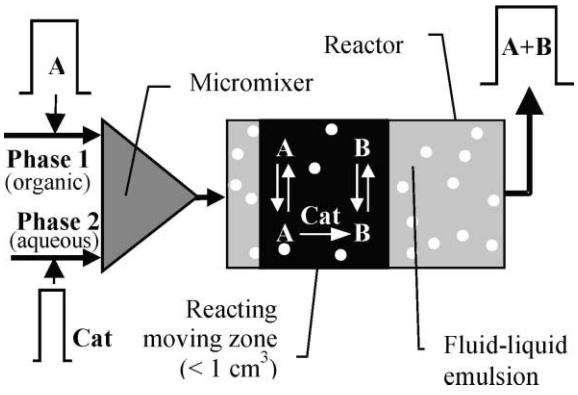

Fig. 12. Principle of a possible set-up for fast sequential fluid–liquid catalyst screening.

Acknowledgements

The authors are grateful to the Région Rhône-Alpes, to the CNRS, to the Ecole Superieure de Chimie Physique Electronique de Lyon (ESCPE) and to the Rhône–Poulenc Company for financial support. The Institut für Microtechnik Mainz (IMM) is greatly acknowledge for the generous loan of the microdevices. The Ph.D. of SC was supported by a grant from the French Ministry of Education. Many thanks also are to Daniel Schweich for fruitful discussions on this work.

References

[1] B. Jandeleit, D.J. Schaefer, T.S. Powers, H.W. Turner, W.H. Weinberg, Angew. Chem. Int. Ed. 38 (1999) 2494.
[2] R.H. Crabtree, Chemtech 29 (4) (1999) 21.
[3] S.R. Gilbertson, X. Wang, Tetrahedron Lett. 36 (1996) 6475.
[4] M.B. Francis, N.S. Finney, E.N. Jacobsen, J. Am. Chem. Soc. 118 (1996) 8983.
[5] K.D. Shimizu, M.L. Snapper, A.H. Hoveyda, Chem. Eur. J. 4 (1998) 1885.
[6] B. Cornils, W.A. Herrmann, in: Applied Homogeneous Catalysis with Organometallic Compounds, VCH, Weinheim, 1996.
[7] B. Cornils, E. Kuntz, J. Organomet. Chem. 502 (1995) 177.
[8] Y. Chauvin, S. Einloft, H. Olivier, Ind. Eng. Chem. Res. 34 (1995) 1149.
[9] I.T. Horvàth, J. Rabai, Science 266 (1994) 72.
[10] R.A. Sànchez-Delgado, M. Rosales, Coord. Chem. Rev. 196 (2000) 249.
[11] C. de Bellefon, N. Tanchoux, Tetrahedron: asymmetry 9 (1998) 3677.
[12] C.R. Landis, J. Halpern, J. Am. Chem. Soc. 109 (1987) 1746.
[13] H.-U. Blaser, H.-P. Jalett, M. Garland, M. Studer, H. Thies, A. Wirth-Tijani, J. Catal. 173 (1998) 282.
[14] M. Bodmer, T. Mallat, A. Baiker, in: F.E. Herkes (Ed.), Catalysis of Organic Reactions, Dekker, New York, 1998, p. 75.
[15] S. Wang, F. Kienzle, Org. Process. Res. Dev. 2 (1998) 226.
[16] Y. Sun, R.N. Landau, J. Wang, C. LeBlond, D. Blackmond, J. Am. Chem. Soc. 118 (1996) 1348.

[17] C. de Bellefon, D. Schweich, N. Tanchoux, in: Proceedings of the Second European Congress on Chemical Engineering, Montpellier, 1999, Preprints on CDROM www.cpc.fr/p_{gpc}.
[18] C. Joly-Vuillemin, D. Gavroy, G. Cordier, C. de Bellefon, H. Delmas, Chem. Eng. Sci. 49 (1994) 4839.
[19] J. Villermaux, in: A. Rodrigues, D. Tondeur (Eds.), Percolation Processes: Theory and Applications, Sijthoff and Noordhoff, Alphen aan den Rijn, 1981, p. 539.
[20] Y. Ito, J. Chromatogr. 538 (1991) 3.
[21] C. de Bellefon, S. Caravieilhes, N. Tanchoux, J. Organomet. Chem. 567 (1998) 143.
[22] C. de Bellefon, S. Caravieilhes, C. Joly-Vuillemin, D. Schweich, A. Berthod, Chem. Eng. Sci. 53 (1998) 71.
[23] N.A. Katsanos, R. Thede, F. Roubani-Kalantzopoulou, J. Chromatogr. A 795 (1998) 133 and references therein.
[24] W. Ehrfeld, H. Löwe, V. Hessel, Th. Richter, Chem. Ing. Technol. 69 (1997) 931.
[25] W. Ehrfeld, K. Golbig, V. Hessel, H. Löwe, Th. Richter, Ind. Eng. Chem. Res. 38 (1999) 1075.
[26] C. de Bellefon, N. Tanchoux, S. Caravieilhes, P. Grenouillet, V. Hessel, Angew. Chem. Int. Ed. 39 (2000) 3442–3445.
[27] M.B. Francis, E.N. Jacobsen, Angew. Chem. Int. Ed. 38 (1999) 937.
[28] J. Villermaux, J. Chromatogr. 406 (1987) 11.
[29] C. de Bellefon, N. Tanchoux, S. Caravieilhes, D. Schweich, Catal. Today 48 (1999) 211.
[30] O. Wörz, K.-P. Jäckel, Th. Richter, A. Wolf, in: Proceedings of the Second International Conference on Microreact. Technology, New Orleans, AIChE Preprints, 1998 183.
[31] V. Hessel, W. Ehrfeld, K. Golbig, V. Haverkamp, H. Löwe, Th. Richter, in: Proceedings of the Second International Conference on Microreact. Technology, New Orleans, AIChE Preprints, 1998, p. 259.